DOI: 10.1002/anie.201310135

Nanotechnology

# A Synergistic Capture Strategy for Enhanced Detection and Elimination of Bacteria**

*Yong-Qiang Li, Bowen Zhu, Yuangang Li, Wan Ru Leow, Rubayn Goh, Bing Ma, Eileen Fong, Mark Tang, and Xiaodong Chen**

***Abstract:*** *Despite the advanced detection and sterilization techniques available today, the sensitive diagnosis and complete elimination of bacterial infections remain a significant challenge. A strategy is reported for efficient bacterial capture (ca. 90%) based on the synergistic effect of the nanotopography and surface chemistry of the substrate on bacterial attachment and adhesion. The outstanding bacterial-capture capability of the functionalized nanostructured substrate enables rapid and highly sensitive bacterial detection down to trace concentrations of pathogenic bacteria (10 colony-forming units $mL^{-1}$). In addition, this synergistic biocapture substrate can be used for efficient bacterial elimination and shows great potential for clinical antibacterial applications.*

The detection and elimination of pathogenic bacteria is central to overcoming bacterial threats, such as foodborne illnesses, hospital-acquired infections, and bioterrorism.[1] Several exquisite platforms that enable the selective detection or elimination of bacterial pathogens have been developed to combat bacterial infections.[2] These platforms, all contain a bacteria-targeting system that enables selective bacterial capture, a capability that is prerequisite for subsequent bacterial detection or elimination.[3] Typically, each bacteria-targeting system is composed of a microfluidic device, nanometer-sized particle, or scaffold conjugated to high affinity synthetic small molecules or antibodies to bind to specific surface biomarkers on bacteria.[2] Although rapid and selective bacterial capture has been achieved by using these bacteria-targeting systems, their low bacterial-capture efficiency limits the clinical applications. The sensitive detection of bacterial pathogens with these systems would be difficult, especially in situations involving extremely low bacteria concentrations, such as sepsis resulting from bacterial pathogen contamination of the bloodstream.[2a,c] To address this issue, bacteria-targeting platforms with outstanding capture efficiency should be developed.

Research into bacterial adhesion during biofilm formation may provide insight into potential strategies for improving bacterial-capture efficiency. The adhesion of bacteria to human tissue or biomaterial surfaces, the first step of biofilm formation, is a synergistic process in which chemical components of the bacterial surface (e.g., proteins and lipopolysaccharides) and extracellular organelles (i.e., flagella and pili) work together to facilitate and achieve bacterial attachment.[4] With this in mind, a strategy could be developed for improving bacterial-capture efficiency by synergistically promoting the interaction between capture platforms and both the chemical components of the bacterial surface and extracellular organelles. However, the element of bacterial extracellular organelles has been neglected in previous designs of bacterial-capture platforms.[2,3] Hence, increasing the interactions between bacterial extracellular organelles and capture platforms becomes a key point for improving capture efficiency. Meanwhile, nanostructures have been reported to have a significant impact on the behavior of bacterial and mammalian cells as a result of local topographic interactions between the nanostructures and nanoscale extracellular organelles,[5,6] and chemically functionalized nanostructures have been used for cancer research.[6] Therefore, we hypothesized that by combining nanotopography and surface chemical modification in the design of bacterial-capture platforms, a synergistic strategy for excellent bacterial capture could be developed.

Herein, we demonstrate a synergistic strategy for enhanced bacterial capture based on a functionalized 3D nanowire substrate. Surface chemical modification of the 3D nanowire substrate is responsible for selective bacterial recognition, while the nanowire topography assists the interaction between the substrate and bacterial extracellular organelles (Scheme S1 in the Supporting Information). The synergistic effect of nanowire topography and surface chemical modification increases bacterial attachment and improves the efficiency of bacterial capture. The enhanced efficiency of bacterial capture of this functionalized 3D nanowire substrate can enable the sensitive detection and efficient elimination of bacterial pathogens.

The 3D functionalized nanowire substrates were prepared as illustrated in Figure 1. Since a large spacing (micrometer) between nanowires would weaken the interactions between nanoscale bacterial extracellular organelles and the nanowires,[4b,5b] we fabricated 3D nanowire substrates with densely packed nanowire arrays on silicon wafers by using silver-assisted chemical etching (Figure 1a).[7] Scanning electron

[*] Dr. Y.-Q. Li, B. Zhu, Dr. Y. Li, W. R. Leow, R. Goh, Dr. B. Ma, Prof. E. Fong, Prof. X. Chen
School of Materials Science and Engineering
Nanyang Technological University
50 Nanyang Avenue, Singapore 639798 (Singapore)
E-mail: chenxd@ntu.edu.sg
Homepage: http://www.ntu.edu.sg/home/chenxd/
Dr. M. Tang
National Skin Centre Singapore
1 Mandalay Road, Singapore 308205 (Singapore)

[**] This work was supported by the Singapore National Research Foundation (CREATE Programme of Nanomaterials for Energy and Water Management and NRF-RF2009-04).

Supporting information for this article is available on the WWW under http://dx.doi.org/10.1002/anie.201310135.

  

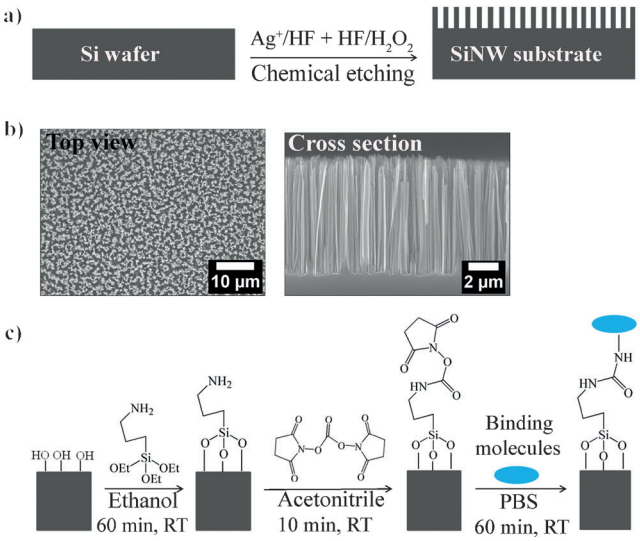


***Figure 1.*** a) A schematic of the 3D SiNW substrate fabrication, which is based on silver-assisted chemical etching. b) SEM images of a typical SiNW substrate. c) Surface chemical modification of the silicon substrates (including SiNW and flat silicon) with bacteria-binding molecules.

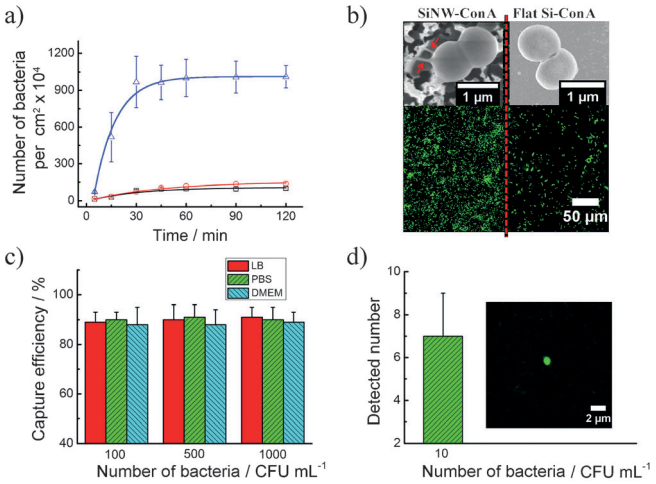


***Figure 2.*** a) Quantitative evaluation of the bacterial-capture yields at different capture times for three different substrates: SiNW (black □), flat Si-ConA (red ○), and SiNW-ConA (blue △). b) Representative fluorescence and SEM images of the ConA-modified patterned substrates with alternate flat and SiNW surfaces after bacterial capture. Nanoscale protrusions (red arrows) were clearly observed between the bacteria and the nanowires in the SEM image, thus indicating enhanced topographical interactions between the nanowires and bacterial extracellular organelles. c) Bacterial-capture efficiency of the SiNW-ConA substrate at different bacteria numbers ranging from 100–1000 CFU $mL^{-1}$ in three different types of sample medium. The capture efficiency is defined as the proportion of bacteria captured from the test sample, and the growth of bacteria in the three media was investigated in the calculation of capture efficiency shown in Figure S5. d) Assay of the SiNW-Con A substrate for highly sensitive bacterial detection with ultra-low bacterial concentrations. The inset fluorescence image shows one of the bacteria captured on the substrate. In (a), (c), and (d), the values for capture efficiency and bacteria numbers represent the mean of three independent experiments and the error bars indicate the standard deviation (SD) from the mean.

microscopy (SEM) images of the resultant substrate revealed that the obtained silicon nanowires (SiNWs) possessed diameters between 100–250 nm and lengths of around 8 μm, and the density of the nanowires is about 15 per $\mu m^2$ (Figure 1b). The spacing between the nanowire structures was between 150 and 400 nm, which is smaller than the diameter scale of a bacterium (submicrometer). Next, bacteria-binding molecules were introduced onto the prepared SiNW substrates through sequential chemical covalent coupling to confer the capability for selective bacterial recognition (Figure 1c and Figure S1 in the Supporting Information).[8]

To evaluate the bacterial-capture performance of the functionalized 3D SiNW substrate, the separation of a bacterial suspension was carried out. *Staphyloccus aureus*, arguably the most prevalent pathogen in humans,[9] was chosen as the model bacterium. Concanavalin A (ConA) was employed for the surface chemical modification of the SiNW substrates because of its high affinity for bacterial lipopolysaccharide components.[10] As shown in Figure 2a, the ConA functionalized 3D SiNW (SiNW-ConA) substrate could capture up to ten times more bacteria than the flat silicon-ConA substrate within short incubation times (30 min), thus indicating the critical role of the nanowire topography in enhanced bacterial capture. Moreover, minimal nonspecific interactions were present between the bacteria and the SiNW substrates in the absence of any surface modification, thus indicating the synergistic effect of nanowire topography and surface bacterial binding molecules for improved bacterial capture. A consistent result was also obtained when using a patterned substrate with alternate flat silicon and SiNW surfaces to provide a spatially close comparison with regards to the bacterial affinity of the functionalized SiNW and flat silicon substrates (Figure 2b and Figure S2). Furthermore, enhanced topographical interactions between the nanowire and the bacteria were found in the SiNW-ConA substrate (Figure 2b, Figure S3 and S4), thus providing further support for our hypothesis. Since the bacterial concentration used in the above tests was very high ($4 \times 10^8$ colony-forming units (CFU) $mL^{-1}$), the performance of the functionalized SiNW substrate for bacterial capture in cases of low bacterial concentrations, as well as the effect of the medium on the capture efficiency, were examined. As shown in Figure 2c, the SiNW-ConA substrate exhibited higher bacterial-capture efficiency (around 90%) at low bacterial concentrations ranging from 100–1000 bacteria $mL^{-1}$ in three different types of medium, thus indicating the flexibility of this substrate with regards to highly efficient bacterial capture and isolation from different clinical samples. The enhanced bacterial capture ability of the SiNW-ConA substrate makes it possible to detect low concentrations of bacteria with high sensitivity and is advantageous for clinical bacterial detection. For our assay with the SiNW-ConA substrate, it was found that an average of seven bacteria was detected under trace concentration conditions (10 CFU $mL^{-1}$; Figure 2d), thus indicating the great potential of this substrate with respect to highly sensitive bacterial detection.

In addition to sensitive bacterial detection, we hypothesized that this synergistic bacterial capture strategy could benefit efficient bacterial elimination. To demonstrate this, a bactericidal assay was designed that makes use of our functionalized 3D SiNW substrate. The bacteria-binding molecule lysozyme was chosen because of its dual functions of efficient bacterial capture and hydrolysis of the bacterial cell wall.[11] As shown in Figure 3a, the lysozyme-functionalized 3D SiNW (SiNW-lysozyme) substrate was found to exhibit highly efficient bacterial killing compared to the flat

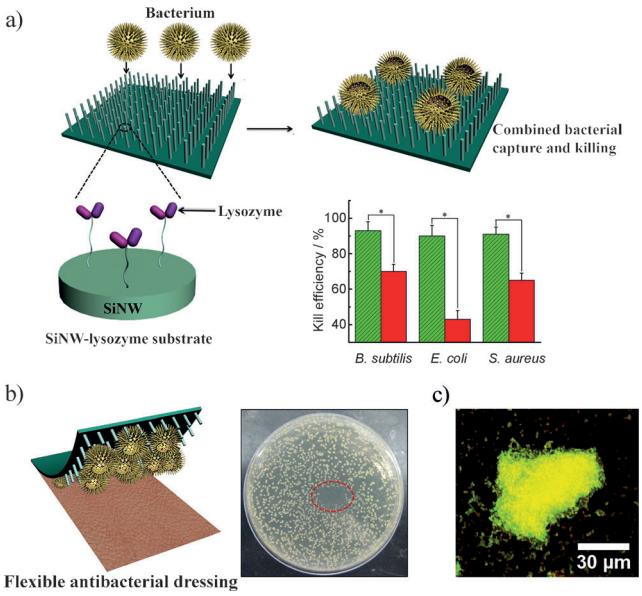


***Figure 3.*** a) A demonstration of the efficient broad-spectrum bactericidal activity of the 3D SiNW-lysozyme substrate. The lysozyme was attached to the end of SiNW nanowires (green bars) or flat silicon (red bars). The killing efficiency values are given as the mean of three independent experiments and the error bars indicate the SD from the mean. $*P<0.05$. b) A demonstration of the potential of the flexible SiNW-lysozyme substrate as an antibacterial dressing. The photograph of the *S. aureus* agar plate was taken after the flexible SiNW-lysozyme substrate had been peeled off. c) A representative LIVE/DEAD bacterial assay of *S. aureus* captured by the flexible SiNW-lysozyme substrate from agar plates. The yellow color, which is due to the overlapping of fluorescence of SYTO 9 (green) and propidium iodide (red), indicates dead bacteria.

silicon-lysozyme substrate based on the results of LIVE/DEAD bacterial assays (Figure S6 and S7). This result was consistent with that of the bacterial capture experiment in which the SiNW-lysozyme substrate also showed higher capture efficiency than the flat silicon-lysozyme substrate (Figure S8). Although the outer membrane structure of gram-negative bacteria would theoretically hinder the interaction between the bacterial cell wall and lysozyme, as well as the subsequent cell wall hydrolysis,[11] the SiNW-lysozyme substrate exhibited high bacterial capture efficiency (51%) for the gram-negative bacterium *Escherichia coli*: 90% of the captured *E. coli* were killed (Figure S8 and Figure 3a). Such a phenomenon may be related to the biophysical bactericidal activity of nanowires towards the outer membrane of gram-negative bacteria,[12] an effect that could provide lysozyme with access to the bacterial cell wall (Figure S9). The combined broad-spectrum bacterial capture and killing ability of the SiNW-lysozyme substrate indicates that it is a good candidate for the clinical treatment of bacterial infections. To this end, we prepared a flexible SiNW-lysozyme substrate (Figure S10) and investigated its potential for the treatment of skin or wound bacterial infections. To simulate the conditions of skin or wound infections, agar plates covered by growing bacterial colonies were employed in our experiments. By affixing the flexible SiNW-lysozyme substrate onto the bacterial agar plate, subjecting it to 6 h of incubation, and then removing the substrate, the ability of the SiNW-lysozyme substrate to eliminate bacteria from agar plates was tested. As shown in Figure 3b, colonies of *S. aureus* within the area covered by the SiNW-lysozyme substrate were found to be efficiently removed from the agar plate. Moreover, the *S. aureus* bacteria captured by the flexible SiNW-lysozyme substrate were discovered to be efficiently killed, as indicated by the results of a LIVE/DEAD bacterial assay (Figure 3c) and SEM investigation (Figure S11). Similar results were obtained when the target bacterium was switched to *Bacillus subtilis* or *E. coli* (Figure S12 and S13), thus demonstrating the great potential of the SiNW-lysozyme substrate as an antibacterial dressing.

This synergistic bacterial capture strategy can be easily combined with controllable bactericidal approaches, such as photodynamic and photothermal therapy,[13] to achieve on-demand bacterial elimination. To demonstrate this, selective *S. aureus* capture and on-demand killing was performed as an example. SiNW substrate modified with human immunoglobulin G (IgG) molecules (SiNW-IgG) was used for selective *S. aureus* capture because of the high affinity of the IgG for protein A, which is expressed uniquely on the cell wall of *S. aureus* (Figure 4a,b).[14] By combining the SiNW-IgG substrate with photodynamic therapy, we proposed a strategy for on-demand *S. aureus* killing. As illustrated in Figure 4c, protein A only binds to the Fc region of the IgG,[14] thus leaving the Fab region of the IgG available for further modification. *S. aureus* killing can thus be achieved by using a secondary-antibody-bound photosensitizer, rose bengal, which generates reactive oxygen species upon light irradiation, thereby killing proximate captured *S. aureus*. As shown in Figure 4d, the round *S. aureus* selectively captured on the SiNW-IgG substrate had clear edges and smooth bodies prior irradiation. After irradiation, the membranes of the *S. aureus* were discovered to have collapsed and merged, thus confirming the death of the bacteria. The killing efficiency of this assay was about 94% (Figure S14).

In conclusion, we report a strategy for bacterial capture based on a functionalized 3D SiNW substrate, which exhibits outstanding bacterial-capture performance as a result of the synergistic effect of the packed nanowire structure and the surface chemical modifications. The excellent bacterial-capture ability of the functionalized 3D SiNW substrate enables the highly sensitive detection and efficient elimination of bacterial pathogens. This substrate thus exhibits great potential for use in clinical antibacterial applications. Our strategy relies on the specific surface chemistry of the nanowire

  

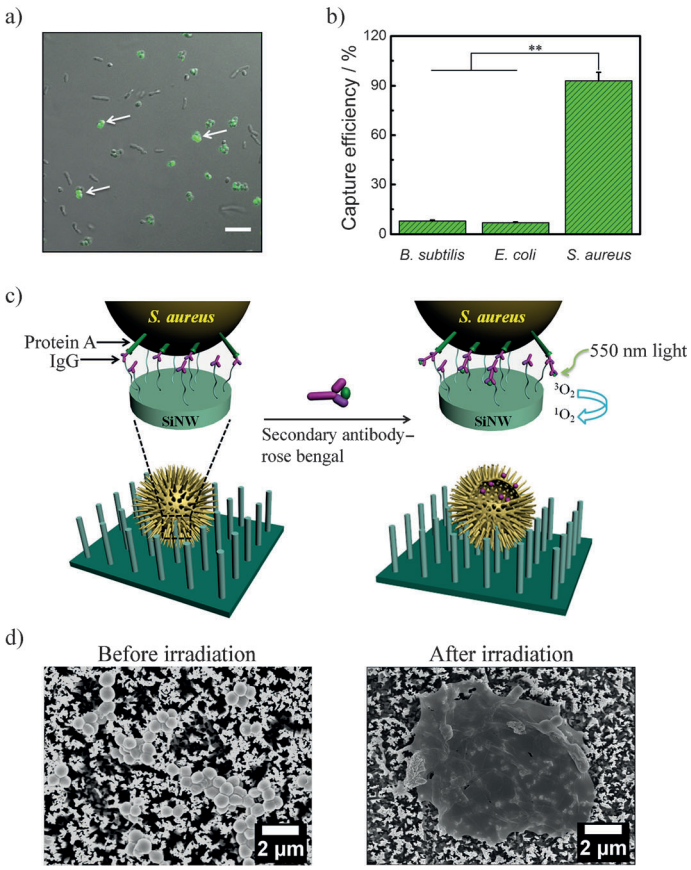


***Figure 4.*** a) Overlapping bright field and fluorescence microscopy images showing the selective interaction between the IgG molecules and *S. aureus*. Only the round *S. aureus* (white arrows) were fluorescently labeled in a mixed culture of *B. Subtilis*, *E. coli* and *S. aureus*. Scale bar: 10 μm. b) The difference in the bacterial capture efficiency of the 3D SiNW-IgG substrate for *B. subtilis*, *E. coli* and *S. aureus* bacteria. The capture efficiency values are given as the mean of three independent experiments and the error bars indicate the SD from the mean. $^{**}P < 0.01$. c) A schematic illustration of on-demand *S. aureus* capture and elimination by using the 3D SiNW-IgG substrate. d) Representative SEM images of *S. aureus* selectively captured on the SiNW-IgG substrate before and after light irradiation.

substrate for bacterial capture; as a result, sensitive bacterial detection may be a challenge in extremely complex systems in which numerous extracellular materials may passivate the nanotopography and/or the chemical modifications on SiNW surface.

Received: November 21, 2013
Revised: January 23, 2014
Published online: March 19, 2014

**Keywords:** antimicrobial agents · bacterial detection · nanotechnology · silicon · surface chemistry

[1] a) C. A. Batt, *Science* **2007**, *316*, 1579–1580; b) A. Y. Peleg, D. C. Hooper, *N. Engl. J. Med.* **2010**, *362*, 1804–1813; c) P. H. Gilligan, *Curr. Opin. Microbiol.* **2002**, *5*, 489–495; d) S. Yin, Y. Goldovsky, M. Herzberg, L. Liu, H. Sun, Y. Zhang, F. Meng, X. Cao, D. D. Sun, H. Chen, A. Kushmaro, X. Chen, *Adv. Funct. Mater.* **2013**, *23*, 2972–2978.

[2] a) T.-Y. Liu, K.-T. Tsai, H.-H. Wang, Y. Chen, Y.-H. Chen, Y.-C. Chao, H.-H. Chang, C.-H. Lin, J.-K. Wang, Y.-L. Wang, *Nat. Commun.* **2011**, *2*, 538; b) J. Gao, L. Li, P.-L. Ho, G. C. Mak, H. Gu, B. Xu, *Adv. Mater.* **2006**, *18*, 3145–3148; c) R. L. Phillips, O. R. Miranda, C.-C. You, V. M. Rotello, U. H. F. Bunz, *Angew. Chem.* **2008**, *120*, 2628–2632; *Angew. Chem. Int. Ed.* **2008**, *47*, 2590–2594; d) J.-J. Lee, K. J. Jeong, M. Hashimoto, A. H. Kwon, A. Rwei, S. A. Shankarappa, J. H. Tsui, D. S. Kohane, *Nano Lett.* **2014**, *14*, 1–5.

[3] a) S. K. Choi, A. Myc, J. E. Silpe, M. Sumit, P. T. Wong, K. McCarthy, A. M. Desai, T. P. Thomas, A. Kotlyar, M. M. B. Holl, B. G. Orr, J. R. Baker, *ACS Nano* **2013**, *7*, 214–228; b) C. Mao, A. Liu, B. Cao, *Angew. Chem.* **2009**, *121*, 6922–6943; *Angew. Chem. Int. Ed.* **2009**, *48*, 6790–6810.

[4] a) Y. Chao, T. Zhang, *Langmuir* **2011**, *27*, 11545–11553; b) L. D. Renner, D. B. Weibel, *MRS Bull.* **2011**, *36*, 347–355; c) H. H. Tuson, D. B. Weibel, *Soft Matter* **2013**, *9*, 4368–4380; d) K. A. Kline, K. W. Dodson, M. G. Caparon, S. J. Hultgren, *Trends Microbiol.* **2010**, *18*, 224–232.

[5] a) R. S. Friedlander, H. Vlamakis, P. Kim, M. Khan, R. Kolter, J. Aizenberg, *Proc. Natl. Acad. Sci. USA* **2013**, *110*, 5624–5629; b) A. I. Hochbaum, J. Aizenberg, *Nano Lett.* **2010**, *10*, 3717–3721; c) J. F. Schumacher, M. L. Carman, T. G. Estes, A. W. Feinberg, L. H. Wilson, M. E. Callow, J. A. Callow, J. A. Finlay, A. B. Brennan, *Biofouling* **2007**, *23*, 55–62; d) L. C. Hsu, J. Fang, D. A. Borca-Tasciuc, R. W. Worobo, C. I. Moraru, *Appl. Environ. Microbiol.* **2013**, *79*, 2703–2712; e) L. Rizzello, B. Sorce, S. Sabella, G. Vecchio, A. Galeone, V. Brunetti, R. Cingolani, P. P. Pompa, *ACS Nano* **2011**, *5*, 1865–1876; f) S. D. Puckett, E. Taylor, T. Raimondo, T. J. Webster, *Biomaterials* **2010**, *31*, 706–713; g) H. E. Jeong, I. Kim, P. Karam, H.-J. Choi, P. Yang, *Nano Lett.* **2013**, *13*, 2864–2869; h) Y.-L. Wu, N. Putcha, K. W. Ng, D. T. Leong, C. T. Lim, S. C. J. Loo, X. Chen, *Acc. Chem. Res.* **2013**, *46*, 782–791; i) C. Y. Tay, P. Cai, M. I. Setyawati, W. Fang, L. P. Tan, C. H. L. Hong, X. Chen, D. T. Leong, *Nano Lett.* **2014**, *14*, 83–88.

[6] a) P. Zhang, L. Chen, T. Xu, H. Liu, X. Liu, J. Meng, G. Yang, L. Jiang, S. Wang, *Adv. Mater.* **2013**, *25*, 3566–3570; b) H. Liu, X. Liu, J. Meng, P. Zhang, G. Yang, B. Su, K. Sun, L. Chen, D. Han, S. Wang, L. Jiang, *Adv. Mater.* **2013**, *25*, 922–927; c) H. Liu, Y. Li, K. Sun, J. Fan, P. Zhang, J. Meng, S. Wang, L. Jiang, *J. Am. Chem. Soc.* **2013**, *135*, 7603–7609; d) S. Yin, Y.-L. Wu, B. Hu, Y. Wang, P. Cai, C. K. Tan, D. Qi, L. Zheng, W. R. Leow, N. S. Tan, S. Wang, X. Chen, *Adv. Mater. Int.* **2014**, *1*, 1300043.

[7] a) K.-Q. Peng, Y.-J. Yan, S.-P. Gao, J. Zhu, *Adv. Mater.* **2002**, *14*, 1164–1167; b) S. Wang, H. Wang, J. Jiao, K.-J. Chen, G. E. Owens, K. Kamei, J. Sun, D. J. Sherman, C. P. Behrenbruch, H. Wu, H.-R. Tseng, *Angew. Chem.* **2009**, *121*, 9132–9135; *Angew. Chem. Int. Ed.* **2009**, *48*, 8970–8973.

[8] a) N. Massad-Ivanir, G. Shtenberg, A. Tzur, M. A. Krepker, E. Segal, *Anal. Chem.* **2011**, *83*, 3282–3289; b) N. Zhang, Y. Deng, Q. Tai, B. Cheng, L. Zhao, Q. Shen, R. He, L. Hong, W. Liu, S. Guo, K. Liu, H.-R. Tseng, B. Xiong, X.-Z. Zhao, *Adv. Mater.* **2012**, *24*, 2756–2760.

[9] a) C. Weidenmaier, J. F. Kokai-Kun, S. A. Kristian, T. Chanturiya, H. Kalbacher, M. Gross, G. Nicholson, B. Neumeister, J. J. Mond, A. Peschel, *Nat. Med.* **2004**, *10*, 243–245; b) D. Bhattacharya, S. P. Chakraborty, A. Pramanik, A. Baksi, S. Roy, T. K. Maiti, S. K. Ghosh, P. Pramanik, *J. Mater. Chem.* **2011**, *21*, 17273–17282; c) C. Paquet, S. Ryan, S. Zou, A. Kell, J. Tanha, J. Hulse, L.-L. Tay, B. Simard, *Chem. Commun.* **2012**, *48*, 561–563.

[10] a) F. A. Jaipuri, B. Y. M. Collet, N. L. Pohl, *Angew. Chem.* **2008**, *120*, 1731–1734; *Angew. Chem. Int. Ed.* **2008**, *47*, 1707–1710; b) M. K. Müller, L. Brunsveld, *Angew. Chem.* **2009**, *121*, 2965–2968; *Angew. Chem. Int. Ed.* **2009**, *48*, 2921–2924; c) S.

Campuzano, J. Orozco, D. Kagan, M. Guix, W. Gao, S. Sattayasamitsathit, J. C. Claussen, A. Merkoci, J. Wang, *Nano Lett.* **2012**, *12*, 396 – 401.

[11] a) H. R. Luckarift, M. B. Dickerson, K. H. Sandhage, J. C. Spain, *Small* **2006**, *2*, 640 – 643; b) A. Pellegrini, U. Thomas, R. von Fellenberg, P. Wild, *J. Appl. Bacteriol.* **1992**, *72*, 180 – 187.

[12] a) S. Pogodin, J. Hasan, V. A. Baulin, H. K. Webb, V. K. Truong, T. H. P. Nguyen, V. Boshkovikj, C. J. Fluke, G. S. Watson, J. A. Watson, R. J. Crawford, E. P. Ivanova, *Biophys. J.* **2013**, *104*, 835 – 840; b) E. P. Ivanova, J. Hasan, H. K. Webb, G. Gervinskas, S. Juodkazis, V. K. Truong, A. H. F. Wu, R. N. Lamb, V. A. Baulin, G. S. Watson, J. A. Watson, D. E. Mainwaring, R. J. Crawford, *Nat. Commun.* **2013**, *4*, 2838.

[13] a) K. Liu, Y. Liu, Y. Yao, H. Yuan, S. Wang, Z. Wang, X. Zhang, *Angew. Chem.* **2013**, *125*, 8443 – 8447; *Angew. Chem. Int. Ed.* **2013**, *52*, 8285 – 8289; b) C. A. Strassert, M. Otter, R. Q. Albuquerque, A. Hone, Y. Vida, B. Maier, L. De Cola, *Angew. Chem.* **2009**, *121*, 8070 – 8073; *Angew. Chem. Int. Ed.* **2009**, *48*, 7928 – 7931; c) C. Zhu, Q. Yang, L. Liu, F. Lv, S. Li, G. Yang, S. Wang, *Adv. Mater.* **2011**, *23*, 4805 – 4810; d) P. C. Ray, S. A. Khan, A. K. Singh, D. Senapati, Z. Fan, *Chem. Soc. Rev.* **2012**, *41*, 3193 – 3209; e) S. Wang, A. K. Singh, D. Senapati, A. Neely, H. Yu, P. C. Ray, *Chem. Eur. J.* **2010**, *16*, 5600 – 5606.

[14] K. C. Ho, P. J. Tsai, Y. S. Lin, Y. C. Chen, *Anal. Chem.* **2004**, *76*, 7162 – 7168.

  